

Sensorless Control of a Synchronous Reluctance Motor based on Improved Sliding Mode Control

Xiaoqing Liu, Kaiyuan Liu, Jianyi Li, Xiaoju Zhao

Shenzhen Institute of Information Technology, Shenzhen 518000, China

Abstract

Synchronous Reluctance Motors (SynRM) have shown significant potential in various industrial applications in recent years due to their low cost and compact structure. However, traditional sliding mode control-based speed control systems for SynRM suffer from significant vibrations and poor robustness. This paper proposes an improved sensorless control technique based on sliding mode control for SynRM to mitigate the inherent vibration issues of sliding mode observers. To demonstrate the superiority of the proposed approach, simulations were conducted in MATLAB/Simulink. The results indicate that the improved sliding mode observer can accurately track the rotor position and provide better accuracy and robustness in rotor position estimation.

Keywords

Synchronous Reluctance Motor; Sliding Mode Observer; Sliding Mode Control; Robustness.

1. Introduction

In modern electric motor control systems, the Synchronous Reluctance Motor has gained widespread adoption in various industrial applications due to its high efficiency and high-performance characteristics. The SynRM excels in terms of efficiency and reliability, particularly in applications that demand high control precision and disturbance rejection, such as electric vehicles, medical equipment, and industrial automation. Achieving high-performance control of the SynRM requires precise estimation of the motor's rotor position and speed. Typically, position sensors are used to obtain this information, but this increases system costs and complexity while also introducing the risk of sensor-related failures. Consequently, researchers have been exploring sensorless control methods to reduce costs and enhance reliability.

In terms of control principles, sensorless control algorithms can be categorized into fundamental waveform control and saliency-based control. During the low-speed startup phase of the synchronous reluctance motor, the saliency-based principle is commonly employed for sensorless control. It involves injecting excitation signals such as square waves, sine waves, or triangular waves[1] to activate the motor and subsequently extracting rotor position information from the high-frequency response signals of the motor. In the high-speed operational phase of the motor, the fundamental waveform principle is utilized to estimate the motor's position. This involves designing various observers based on extended back electromotive force (EMF), such as back EMF observers, model reference adaptive control, neural network control, and sliding mode observers[2]. These observers are used to extract the rotor position.

The sliding mode observer is a method based on sliding mode control theory, which, by constructing a sliding surface and tracking the state error, can achieve motor position estimation. Sliding mode observers typically offer excellent robustness and disturbance rejection performance. They have become a significant branch of control theory and find wide applications in various fields, including automotive control and flight control[3]. However, according to the fundamental principles of sliding

mode control, the presence of chattering in sliding mode control can affect control system accuracy. Therefore, eliminating chattering becomes a crucial issue in optimizing sliding mode control.

Some studies have analyzed the causes of chattering in sliding mode control, providing corresponding solutions to enhance sliding mode control performance. Other researchers have incorporated advanced control theories such as adaptive control, neural network control, fuzzy control, and terminal sliding mode into sliding mode control systems to improve control effectiveness and reduce chattering. In terms of the sliding mode observer convergence rate, novel non-linear convergence rates[4] have been proposed and applied to sliding mode speed control for permanent magnet synchronous motors. These convergence rates dynamically adapt to changes in the sliding surface and system state, maintaining the dynamic performance of the sliding mode controller while effectively suppressing chattering. In addition, super-twisting second-order sliding mode and fractional-order sliding mode[5] have been applied to sensorless control systems for permanent magnet synchronous motors and induction motors, effectively reducing chattering without compromising observer robustness. One study[6] proposed an improved sliding mode observer using a combination of exponential convergence law and reverse sine saturation function convergence law, resulting in reduced velocity error compared to traditional sliding mode observers, and an improved solution to the chattering issue.

This paper aims to explore improved sliding mode control strategies and design new control strategies to mitigate chattering, enhance the accuracy of position and velocity estimation, and improve the robustness of the system.

2. Mathematical Model

2.1 Mathematical Model of Synchronous Reluctance Motor

In ideal conditions, the mathematical model of the synchronous reluctance motor can be expressed in the $\alpha\beta$ stationary coordinate system as follows:

$$\begin{bmatrix} \dot{i}_\alpha \\ \dot{i}_\beta \end{bmatrix} = \frac{1}{L_d} \begin{bmatrix} -R_s & -\omega_e(L_d - L_q) \\ \omega_e(L_d - L_q) & -R_s \end{bmatrix} \begin{bmatrix} i_\alpha \\ i_\beta \end{bmatrix} + \frac{1}{L_d} \begin{bmatrix} u_\alpha \\ u_\beta \end{bmatrix} - \frac{1}{L_d} [(L_d - L_q)(\omega_e i_d - p i_q)] \begin{bmatrix} -\sin \theta_e \\ \cos \theta_e \end{bmatrix} \quad (1)$$

In the above equation, u_α , u_β , i_α , and i_β represent the $\alpha\beta$ -axis voltage and current components, R_s is the stator resistance, p denotes the differential operator, ω_e and θ_e correspond to the motor's electrical angular velocity and electrical angle, and L_d and L_q are the direct and quadrature axis inductances, with L_d being significantly larger than L_q in synchronous reluctance motors., Replacing equation (1)

with respect to the $M = \frac{1}{L_d} \begin{bmatrix} -R_s & -\omega_e(L_d - L_q) \\ \omega_e(L_d - L_q) & -R_s \end{bmatrix}$, $N = \frac{1}{L_d}$,

$E = \begin{bmatrix} E_\alpha \\ E_\beta \end{bmatrix} = [(L_d - L_q)(\omega_e i_d - p i_q)] \begin{bmatrix} -\sin \theta_e \\ \cos \theta_e \end{bmatrix}$ coordinate system, the resulting expression is as follows:

$$\begin{bmatrix} \dot{i}_\alpha \\ \dot{i}_\beta \end{bmatrix} = M \begin{bmatrix} i_\alpha \\ i_\beta \end{bmatrix} + N \begin{bmatrix} u_\alpha \\ u_\beta \end{bmatrix} - NE \quad (2)$$

In equation (2), E represents the extended back electromotive force, and it can be observed from the expression of E that it contains information about the rotor's position. Through an appropriate position demodul mode observer for the synchronous reluctance motor is as follows:

2.2 Design of the Sliding Mode Observer

To estimate the rotor position and speed of the motor, the designed sliding mode observer for the synchronous reluctance motor is as follows:

$$\begin{bmatrix} \dot{i}'_{\alpha} \\ \dot{i}'_{\beta} \end{bmatrix} = A \begin{bmatrix} i'_{\alpha} \\ i'_{\beta} \end{bmatrix} + B \begin{bmatrix} u_{\alpha} \\ u_{\beta} \end{bmatrix} - BK \begin{bmatrix} y(\hat{i}_{\alpha}) \\ y(\hat{i}_{\beta}) \end{bmatrix} \quad (3)$$

The system sliding surface is designed as the difference between the observed current of the sliding mode observer and the actual current. Its equation is as follows:

$$s = \begin{bmatrix} \hat{i}_{\alpha} \\ \hat{i}_{\beta} \end{bmatrix} = \begin{bmatrix} i'_{\alpha} - i_{\alpha} \\ i'_{\beta} - i_{\beta} \end{bmatrix} \quad (4)$$

Subtracting equation (3) from equation (2) yields:

$$\begin{bmatrix} \dot{\hat{i}}_{\alpha} \\ \dot{\hat{i}}_{\beta} \end{bmatrix} = A \begin{bmatrix} \hat{i}_{\alpha} \\ \hat{i}_{\beta} \end{bmatrix} + B \begin{bmatrix} E_{\alpha} - Ky(\hat{i}_{\alpha}) \\ E_{\alpha} - Ky(\hat{i}_{\beta}) \end{bmatrix} \quad (5)$$

When $s=0$, the motor control continuously switches on the sliding surface. At this point, $\begin{bmatrix} E_{\alpha} - Ky(\hat{i}_{\alpha}) \\ E_{\alpha} - Ky(\hat{i}_{\beta}) \end{bmatrix} \approx 0$, so the extended back electromotive force can be represented by the designed switching function. The control strategy of the sliding mode observer can be represented by Fig. 1. The back electromotive force obtained through the switching function contains a large amount of high-frequency signals and requires low-pass filtering. Consequently, the estimated value of the extended back electromotive force is:

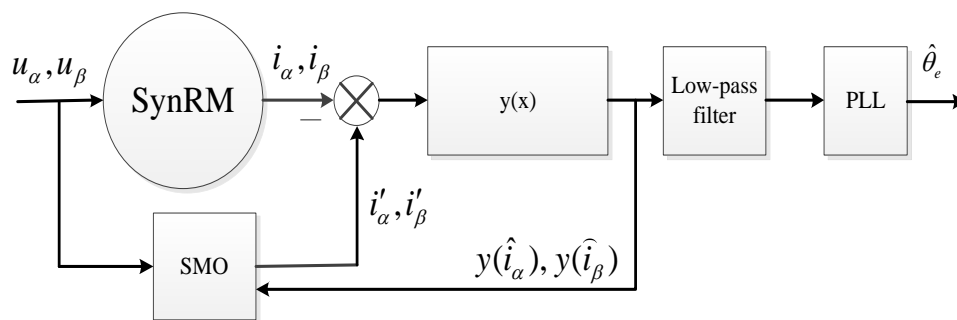


Fig 1 The control strategy of the sliding mode observer

2.3 Improved Sliding Mode Observer Design

In traditional sliding mode observer control algorithms, the use of discontinuous switching functions as sliding mode convergence laws leads to significant vibrations in the motor control system, limiting the industrial application of the algorithm. In this paper, based on the concept of quasi-sliding mode, a new segmented exponential saturation function is designed to replace the traditional switching function in order to reduce vibrations. Its equation is as follows:

$$y(x) = \begin{cases} 1, & x \geq k \\ \frac{\text{sgn}(x)}{k^4} x^4, & -k \leq x \leq k \\ -1, & x < -k \end{cases} \quad (6)$$

In the equation, "k" is the boundary of the control function, and "sgn(x)" is the sign function. Outside the boundary layer, there is switching control with characteristics similar to the sign function, while inside the boundary layer, there is continuous control in exponential form. This continuous control function reduces the speed at which the state variables cross the sliding surface, avoiding high-speed switching of the sign function, and effectively mitigates vibrations. "k" determines the thickness of the boundary layer, and the thickness of the boundary layer directly affects the system's vibration suppression and robustness. Therefore, to improve the vibration suppression effect of the system while ensuring the robustness of the sliding mode, "k" needs to be selected reasonably.

2.4 Phase-Locked Loop (PLL) Rotor Position Identification

During the operation of the motor, due to interference from various harmonics, if rotor position demodulation is directly performed on the signal filtered by a low-pass filter using the arctangent, the estimated motor speed ω_e and θ_e may have significant spikes, potentially leading to system instability. If a low-pass filter is introduced to remove harmonics, it may increase tracking errors. Therefore, this paper employs a Phase-Locked Loop (PLL) for the detection of ω_e and θ_e , thereby improving tracking performance.

To eliminate the influence of amplitude on position demodulation, an orthogonal PLL is used to process the signal. The principle is shown in Fig. 2.

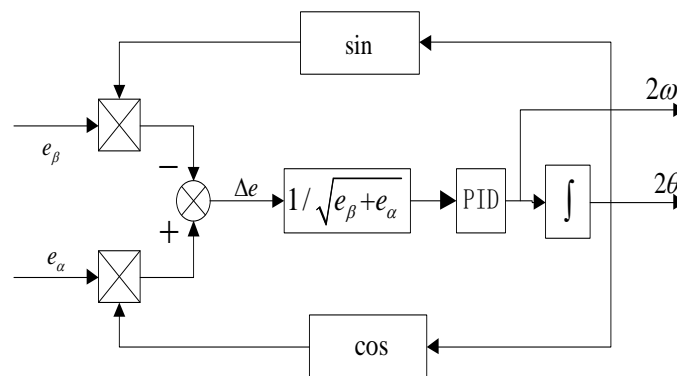


Fig 2 the demodulation diagram of PLL

$$\Delta e = 2kL\Delta L \sin 2(\hat{\theta} - \hat{\theta}_e) \approx 4kL\Delta L \Delta \theta \quad (7)$$

From equation (7), it can be deduced that when $\hat{\theta} - \hat{\theta}_e$ is very small, the phase difference e is adjusted to converge to 0 through a PID controller and an integrator, thus detecting the rotor position.

3. Software Simulation Analysis

Based on the sliding mode observer described in the previous sections, design the control system block diagram for the sensorless control of the SynRM as shown in Figure 7. Subsequently, build a simulation model in the simulation software to perform feasibility verification. Table 1 provides the various parameters of the SynRM model.

Table 1. The parameters of SynRel prototype

ID	Parameters	Unit	Number
1	Rated speed	r/min	3000
2	Rated voltage	V	220
3	Rated power	kW	1.2
4	Rated torque	N•m	4
5	Number of poles		2
6	Resistance	Ω	0.8017
7	Inductance L_d	H	0.0543112
8	Inductance L_q	H	0.0102127
9	Moment of inertia	kg•m ²	0.0007696

Fig. 3 shows the waveform of the extended back electromotive force of the synchronous reluctance motor as it accelerates from 1000 r/min to 1500 r/min and eventually stabilizes at 1500 r/min. From the graph, it can be observed that the extended back electromotive force takes on a sinusoidal waveform. Through demodulation algorithms, rotor position and speed information can be extracted from the sine and cosine wave components.

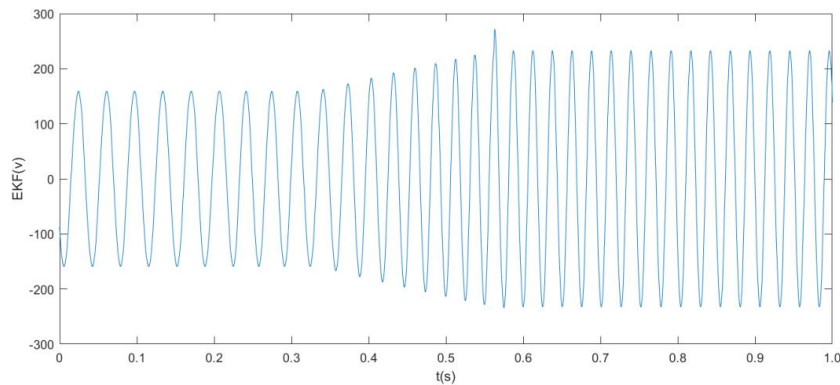


Fig. 3 the waveform of the extended back electromotive force of the SynRM

Fig. 4 displays the waveforms of the position identification and position error of the synchronous reluctance motor's sliding mode control at a speed of 1000 r/min. From the waveforms, it can be observed that the algorithm effectively tracks the actual position of the motor.

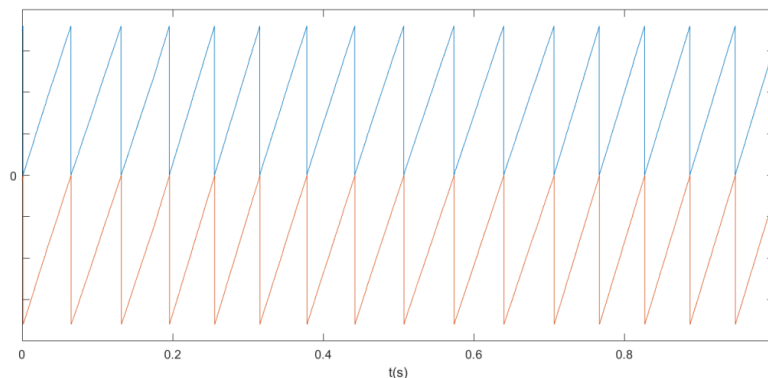


Fig. 4 the waveforms of actual position and estimated position for the SynRM

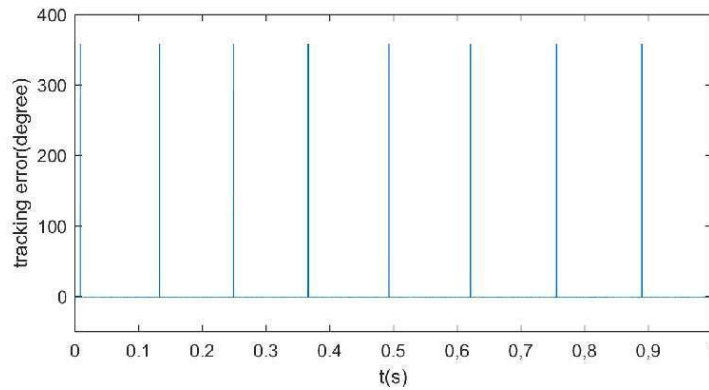
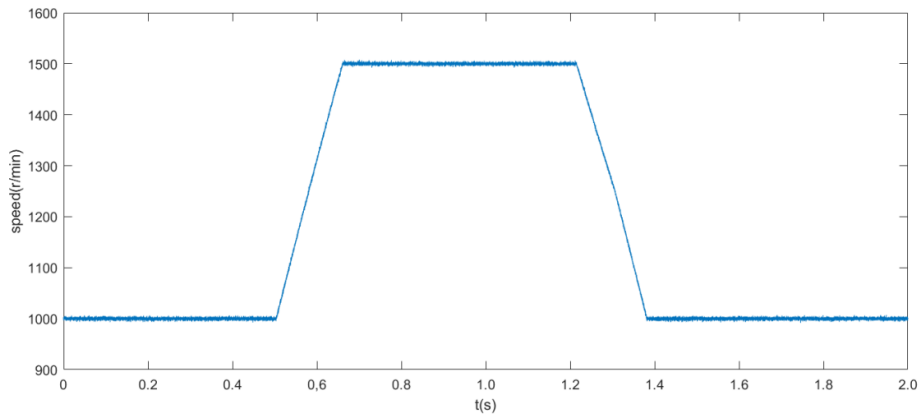
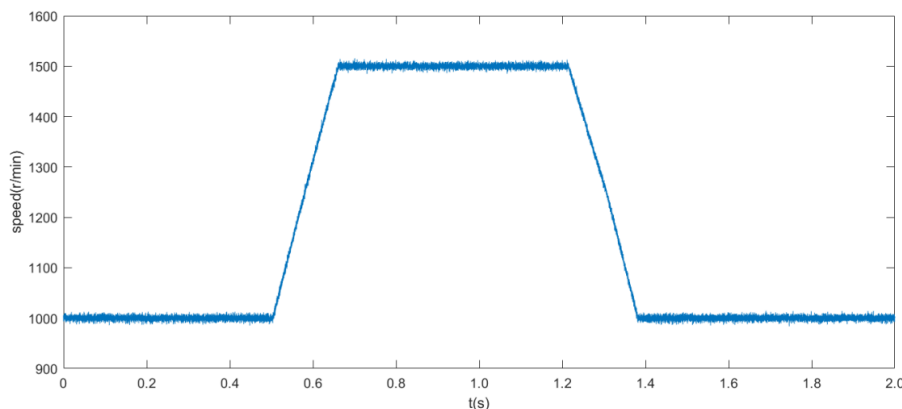


Fig. 5 Rotor Position Tracking Error Waveform

To compare the performance of the improved sliding mode control algorithm and the traditional algorithm, Fig. 6 displays the motor's speed waveforms for both control algorithms. Fig. 6(a) corresponds to the actual speed waveform for the improved sliding mode control algorithm, while Fig. 6(b) corresponds to the actual speed waveform for the traditional control algorithm. The motor accelerates from 1000 r/min to 1500 r/min and then decelerates back to 1000 r/min under synchronous reluctance motor sliding mode control for speed identification. From the waveform in Fig. 6(a), it can be observed that the speed amplitude is smaller, indicating that the algorithm effectively tracks the actual motor position.



(a) actual speed waveform corresponding to improved sliding mode control algorithm



(b) estimated speed waveform corresponding to improved sliding mode control algorithm

Fig. 6 motor speed waveform

4. Conclusion

In this study, we explored the sensorless control strategy for synchronous reluctance motors using sliding mode control. We introduced an improved sliding mode control method with a new sliding mode convergence law. This method effectively mitigates the inherent chattering problem in the system and enhances robustness to external disturbances and uncertainties. Simulation results confirm the advantages of our proposed approach over traditional strategies in terms of response speed, accuracy and robustness.

Acknowledgments

Fund Project: University-level High-high Plan-Innovation Elactor Cultivation Special-Master and Doctor Research Start-up Project (Project No.: SZIIT2022KJ055).

References

- [1] NI R, XU D, BLAABJERG F, et al. Square-wave voltage injection algorithm for PMSM position sensorless control with high robustness to voltage errors[J]. IEEE Transactions on Power Electronics, 2017, 32(7): 5425-5437.
- [2] Jin H Y, Zhao X M, Wang T H. Modified complementary sliding mode control with disturbance compensation for permanent magnet linear synchronous motor servo system[J]. IET Electric Power Applications, 2020, 14(11): 2128-2135.
- [3] H. S. Masood, P. Balachandra, M. Wondimagegn, A. Denekew, C. Bakana, A. Abibual. Sliding Mode Controller for Electric Vehicles based on Switched Boost Converter[J]. Journal of Physics: Conference Series, 2021, 1964(4).1742-1749.
- [4] ZHANG X, SUN L, ZHAO K, et al. Nonlinear speed control for PMSM system using sliding-mode control and disturbance compensation techniques[J]. IEEE Transactions on Power Electronics, 2013, 28(3): 1358-1366.
- [5] Z. Q. Liu, W. K. Chen. Research on an Improved Sliding Mode Observer for Speed Estimation in Permanent Magnet Synchronous Motor[J]. Processes, 2022, 10(6).1182-1186.
- [6] SURYAWANSHI P V, SHENDCE P D, PHADKE S B. A boundary layer sliding mode control design for chatter reduction using uncertainty and disturbance estimator[J]. International Journal of Dynamics and Control, 2016, 4(4):456-465.